HardwareX 9 (2021) e00180

Contents lists available at ScienceDirect

HardwareX

journal homepage: www.elsevier.com/locate/ohx

Hardware Article

TreeMMoSys: A low cost sensor network to measure wind-induced tree response

Sven Kolbe *, Dirk Schindler

Environmental Meteorology, University of Freiburg, Werthmannstrasse 10, D-79085 Freiburg, Germany

ARTICLE INFO

Article history:
Received 15 October 2020
Received in revised form 15 February 2021
Accepted 21 February 2021

Keywords:
Tree response monitoring
Sensor network
Wind-tree interactions
Natural hazards

ABSTRACT

Severe storms caused the largest amount of damaged timber in European forests in the past 70 years. Storm damage occurs when wind loads exceed the failure limits of trees. A decisive factor in assessing storm damage is comprehensive knowledge of interactions between the aerial parts of trees and the high-impact airflow. This paper describes the inexpensive multiple sensor system TreeMMoSys that can measure aerial tree parts' wind-induced reactions, including branches and the stem. The output of TreeMMoSys includes acceleration and angular rate data converted to tilt angles in the post-processing. The system consists of a scalable number of light-weight tree response sensors and ground receivers that communicate through a WLAN network. The weatherproofed system is highly portable, reusable, and allows for an efficient monitoring and a maximization of the number of study trees. Due to the stable measurement performance and accuracy of TreeMMoSys, it can be deployed in the field for long-term monitoring of single tree reactions or neighboring trees' reactions to wind excitation.

Specification table

Hardware name	TreeMMoSys
Subject area	Environmental, forest and agricultural sciences, educational tools
Hardware type	Motion sensor, field measurements, mechanical engineering
Open Source License	GNU General Public License v. 3
Cost of Hardware	275.09€ for a V1 system setup with 10 tree response sensors
Source File Repository	https://doi.org/10.17605/OSF.IO/J63V5

* Corresponding author.
E-mail address: sven.kolbe@meteo.uni-freiburg.de (S. Kolbe).

https://doi.org/10.1016/j.ohx.2021.e00180
2468-0672/

1. Hardware in context

Storms are an essential component of the natural disturbance dynamics of forest ecosystems [1]. In recent decades, they have caused about 53% of the total amount of damaged timber accumulated in European forests [2]. Since catastrophic storms not only disrupt forest operations but also have far-reaching consequences for silviculture, forest protection, ecology, forest administrations, and forest owners have a big interest in minimizing the damage caused by storms and the associated adverse effects. It was also found that a large part of the unexplained interannual variability of the terrestrial CO_2 balance can be explained by storm damage. For example, the high-impact storm Lothar that hit Europe in December 1999 [3] led to an estimated 30% decrease in the European net biome production [4].

Because a large number of trees are regularly damaged by storms, there is great interest in a comprehensive understanding of the processes that contribute to storm damage. Therefore, substantial efforts are being made to understand the formation and patterns of storm damage in forests [5–8] and urban trees better [9,10].

The first step in understanding storm damage to trees is a comprehensive knowledge of the reactions of the aerial tree parts (foliage, branches, stem) exposed to wind loads near the ground. It is important to note that the wind loads have turbulent and non-turbulent components and trees react to both components. The distinction between turbulent and non-turbulent components is often based on the Reynolds decomposition [11], which separates time series of atmospheric flow into turbulent and mean components.

To understand trees' interactions with the near-surface airflow, it is necessary to know their reactions to turbulent and mean components of wind loads. To ensure that the near-surface airflow's essential turbulent properties are captured, turbulence measurements are commonly made at frequencies of 10 Hz and more [12]. Since all near-surface airflow components can potentially induce reactions of the aerial parts of the tree, their responses were also sampled at frequencies of 10 Hz in previous studies [13,14].

Although the above-ground tree architecture and the associated wind-induced reaction behavior of trees are often complex [8], tree reaction measurements have mostly been carried out at single heights on the stem or other vertical main axes of trees. It is assumed that integral reactions, which result from the different vibrational behavior of all above-ground tree parts, can be studied there. To analyze storm damage formation at the tree level, integral tree reactions are often measured close to the stem base to assess the total wind forces acting on the tree parts above and below the ground [15–18].

To date, very few field studies have been carried out on full-scale trees in which multi-sensor systems were used to measure wind loads and the associated reactions of branches and along the stem at several heights simultaneously [19]. One reason for this lack of field studies is inexpensive, ready-to-use multi-sensor systems with an integrated data recording unit were not available.

Here, we describe the tree motion monitoring system TreeMMoSys, a scalable, low-cost multi-sensor system. The system enables the measurements of wind-induced tree reactions known to occur in aerial parts of trees. The system can easily be adapted to individual needs and offers the possibility to use multiple sensors to monitor reactions of tree parts such as branches and the stem of one or more neighboring trees. A previous version of the described system was already used in an earlier field study [14] to measure motion along the stem of a plantation-grown Scots pine (*Pinus sylvestris*) tree at seven heights for five months. Details on the sensor assembly, the recording, and processing of the measured tree response data are presented in this paper.

2. Hardware description

TreeMMoSys combines up to 10 tree response sensors (TRS) and a ground-based receiver to store data from multiple TRS simultaneously. TRS is equipped with an Arduino IDE compatible microcontroller (Wemos D1 mini) and a nine-axis motion-tracking device (MPU-9250 MotionTracking™ Device, InvenSense, USA). TRS and ground receiver communicate through a WLAN network. The MPU-9250 is a combination of a 3-axis accelerometer, 3-axis gyroscope and 3-axis magnetometer and the raw outputs of the sensors are given as acceleration (m/s^2), angular rate (rad/s) and magnetic field strength (μT).

The total weight of one TRS is approximately 27 g. It can be attached to all aerial parts of trees if they are not affected by the sensor's weight. Multiple TRS can be connected to a permanent 5 V power supply to allow long-term monitoring of tree part responses, to reduce overall sensor weight, and to avoid battery charging. Data from TRS has a low variation over temperature and drift over time. Change over temperature given by the manufacturer datasheet of the accelerometer is equal to $\pm 0.118^{-4}$ $(m/s^2)/°C$ and of the gyroscope it is ±0.0042 (rad/s)/°C [20]. Whereas some other methods are restricted to measurements at the stem base, the proposed system can also be used to study whole tree motion for a relatively low hardware price. No additional data cables are needed, only a cable for a permanent power supply of the TRS. The mounting method of individual sensors does not cause damage to the study trees and allows for monitoring of the tree response to wind excitation at remote places without access to the electrical grid. The ground receiver needs no additional coverage. It can be mounted to a pole, the sample tree or an adjacent tree. The straightforward installation of TRS enables a cost-effective monitoring and a maximization of the number of study trees.

2.1. System setup and communication

The Wemos D1 mini is a 32-bit microcontroller with an onboard 2.4 GHz WLAN chip (type ESP8266, Espressif, China). WLAN is used to send tree motion data to a ground-based receiver (type Raspberry Pi Zero W, Raspberry Pi Foundation, UK). The Raspberry Pi is configured as a WLAN access point to enable the one-way data transfer between TRS and the ground receiver using the Message Queuing Telemetry Transport (MQTT) communication protocol. The ground receiver is equipped with a real-time clock (RTC, type DS3231, maxim integrated, CA, US) to allow time synchronization of the system after power interruptions and starting procedures. The ground station adds a time stamp to each data string it receives from a TRS, which is used in post-processing to resample the TRS data and synchronization with the airflow measurements.

2.2. System options and power consumption

Two versions (V1, V2) of TreeMMoSys are available. V1 is used for large trees up to a height of 30 m. It consists of up to 10 TRS, a ground receiver, and an additional WLAN access point (Fig. 1). The ground receiver is equipped with an RTC for synchronizing the measurements, a USB memory stick for data storage, and two switches for a minimum of operator control. The first switch is used to eject the USB memory stick for replacement. The second switch is used to turn off the ground receiver safely.

The maximum distance between the ground receiver and an individual TRS can be 15 m. A WLAN access point can be set up to increase the distance between a TRS and the ground receiver to a maximum of 30 m in one direction. This is especially useful if a TRS is installed higher up in a tree and the distance to the ground receiver extends 15 m. Then, the ground receiver and all TRS are connected to the WLAN access point. Tree response data is routed from TRS over the WLAN access point to the ground receiver and temporarily stored on the ground receiver's internal storage.

V2 is a simplified version of V1. It consists of only TRS and the ground receiver (Fig. 2). The WLAN access point is directly integrated into the ground receiver, so no additional components are necessary. This system setup is recommended when the distance between individual TRS and the ground receiver does not exceed 15 m. This could be the case if smaller trees are studied or multiple adjacent trees within the 15 m WLAN coverage are sampled. There is potential to sample trees outside the 15 m range with V2, but this depends mainly on the local conditions such as stand and vegetation density and the number of TRS connected to the WLAN access point.

An extension of the WLAN range of V1 or V2 may be implemented with any commercially available WLAN repeater. Optionally, one or more Wemos D1 mini can be configured as individual WLAN repeaters. This enables also automesh mode for an optimal network range and functionality. The configuration of the ESP8266 as functional WLAN repeater is described in detail by elsewhere [21,22]. In general, we recommend to use multiple ground receivers/WLAN access points instead of increasing the WLAN coverage by repeaters. Table 1 provides information on the power consumption of each component of V1 and V2.

3. Design files

The design files consist of all 3D printable parts needed to assemble and use TreeMMoSys under outdoor conditions all year round (Table 2).

- *Part_1 Sensor housing,* protects all TRS components from moisture and other environmental influences.
- *Part_2 Lid sensor housing,* allows for the integration of an external power supply.
- *Part_3 Cable cover,* protects the micro USB plug of the external power supply from moisture and other environmental influences.

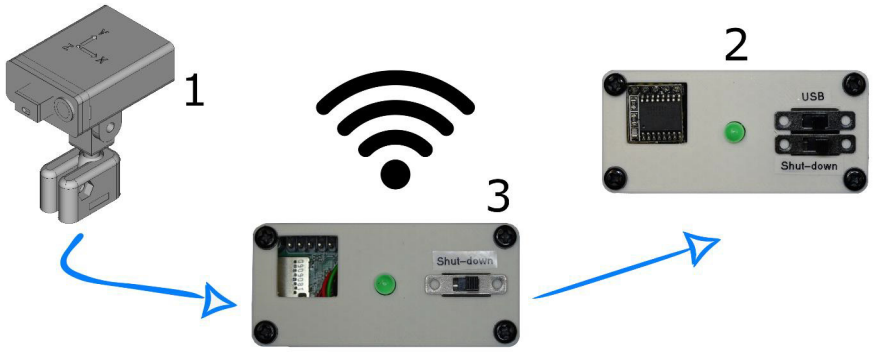

Fig. 1. TreeMMoSys version 1 (V1) consisting of (1) tree response sensors (TRS), (2) ground receiver, and (3) WLAN access point.

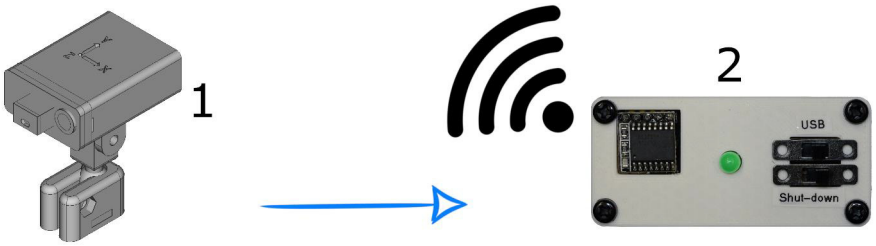

Fig. 2. TreeMMoSys version 2 (V2) consisting of (1) tree response sensor (TRS) and (2) ground receiver.

Table 1
Power consumption (PC) of V1 and V2 running with 1 or 10 TRS per ground receiver.

	Component	PC of 1 TRS	PC of 10 TRS
V1	WLAN access point	0.13 A	0.13 A
	Ground receiver	0.13 A	0.13 A
	TRS	0.03 A	0.32 A
	Total power demand	0.29 A	0.58 A
	Running time on a 12 V 60 Ah battery	≈ **206 h**	≈ **103 h**
V2	Ground receiver	0.13 A	0.13 A
	TRS	0.03 A	0.32 A
	Total power demand	0.16 A	0.45 A
	Running time on a 12 V 60 Ah battery	≈ **375 h**	≈ **133 h**
Optional	Wemos D1 mini as WLAN repeater	0.03 A	0.03 A

Table 2
List of design files.

Design filename	File type	Open source license	Location of the file
Part_1 Sensor housing	3D Model (.stl)	GNU GPL v3.	https://doi.org/10.17605/OSF.IO/J63V5
Part_2 Lid sensor housing	3D Model (.stl)	GNU GPL v3	https://doi.org/10.17605/OSF.IO/J63V5
Part_3 Cable cover	3D Model (.stl)	GNU GPL v3	https://doi.org/10.17605/OSF.IO/J63V5
Part_4 Mount MPU9250	3D Model (.stl)	GNU GPL v3	https://doi.org/10.17605/OSF.IO/J63V5
Part_5 Ball head	3D Model (.stl)	GNU GPL v3	https://doi.org/10.17605/OSF.IO/J63V5
Part_6 Mount base	3D Model (.stl)	GNU GPL v3	https://doi.org/10.17605/OSF.IO/J63V5
Part_7 LED lid	3D Model (.stl)	GNU GPL v3	https://doi.org/10.17605/OSF.IO/J63V5
Part_8 Panel Ground Receiver	3D Model (.stl)	GNU GPL v3	https://doi.org/10.17605/OSF.IO/J63V5
Part_9 Panel WLAN Access Point	3D Model (.stl)	GNU GPL v3	https://doi.org/10.17605/OSF.IO/J63V5

- *Part_4 Mount MPU9250,* aligns the MPU9250 and D1 mini-board.
- *Part_5 Ball head,* allows for an individual alignment and fixation of the sensor.
- *Part_6 Mount base,* used to mount the sensor on stem or individual branches using a cable tie.
- *Part_7 LED lid,* allows the indication LED to be visible from outside (transparent filament).
- *Part_8 Panel ground receiver,* carries the Raspberry Pi Zero W ground receiver.
- *Part_9 Panel WLAN access point,* carries the Raspberry Pi Zero W WLAN access point.

4. Bill of materials

Table 3 lists all materials needed to build TRS. Table 4 specifies all materials required to assemble the ground receiver, including the WLAN access point. A list of additional materials required for the system installation is given in Table 5. The online links of all materials are provided in the Appendix.

5. Build instructions

This section gives instructions on how (1) to assemble TRS, ground receiver, WLAN access point, and power supply, (2) to prepare the software images for the ground receiver and the WLAN access point. Additional photo series for the assembling steps are provided online: https://doi.org/10.17605/OSF.IO/J63V5.

Table 3
Bill of materials required to assemble a tree response sensor (TRS).

ID	Component	Quantity	Unit	Total (€)	Material type
TMS01	D1 Mini - ESP8266	1	4.86	4.86	Electronics
TMS02	GY-9250 module	1	6.34	6.34	Electronics
TMS03	Wire red 0.14 mm^2	0.04 m	0.01	0.04	Non-specific
TMS04	Wire black 0.14 mm^2	0.03 m	0.01	0.04	Non-specific
TMS05	Wire green 0.14 mm^2	0.02 m	0.01	0.03	Non-specific
TMS06	Wire white 0.14 mm^2	0.02 m	0.01	0.03	Non-specific
TMS08	Twin-stranded wire 0.14 mm^2	0.15 m	0.02	0.03	Non-specific
TMS09	Micro USB plug type B	1	0.85	0.85	Non-specific
TMS10	LED green 3 mm	1	0.10	0.10	Electronics
TMS11	Heat-shrink 2.4 mm	0.04 m	0.01	0.04	Non-specific
TMS12	Foam	0.035 m	0.01	0.03	Non-specific
TMS13	Screw M3 × 22 mm	1	0.69	0.69	Metal
TMS14	Screw M3 × 14 mm	1	0.15	0.15	Metal
TMS15	Nut M3	2	0.04	0.08	Metal
TMS16	Washer M3	3	0.04	0.12	Metal
TMS17	ABS filament white (*Part_1* to *Part_6*)	6.67 m	0.15	1.00	ABS
TMS18	ABS filament transparent (*Part_7*)	0.16 m	0.13	0.02	ABS
TMS19	Mibenco® liquid rubber white	2 g	0.08	0.16	Polymer
		Grand total		**14.61** €	

Table 4
Bill of materials required to assemble the ground receiver and the WLAN access point.

ID	Component	Quantity	Unit	Total (€)	Material type
GBR01	Raspberry Pi Zero W	2	18.81	30.38	Electronics
GBR02	MicroSD card 4–8 GB	2	3.61	7.22	Electronics
GBR03	Junction box 100 × 100 × 40 mm	2	0.81	1.62	Non-specific
GBR04	Step down module	2	3.00	6.00	Electronics
GBR05	Heat-shrink 12.8 mm	0.08 m	0.02	0.14	Non-specific
GBR06	Twin-stranded wire 0.75 mm^2	0.2 m	0.04	0.04	Non-specific
GBR07	JST xh 2.5–2 Pin connector	2	0.34	0.68	Non-specific
GBR08	Circuit board	1	0.97	0.97	Non-specific
GBR09	Foam	0.10 m	0.01	0.10	Non-specific
GBR10	Terminal block	1	1.12	1.12	Non-specific
GBR11	RTC DS3231	1	2.25	2.25 s	Electronics
GBR12	USB memory stick 64 GB	1	10.67	10.67	Electronics
GBR13	USB OTG adapter cable	1	1.46	1.46	Non-specific
GBR14	LED Green 5 mm	2	0.10	0.20	Non-specific
GBR15	Resistor 330 Ohm	2	0.15	0.30	Non-specific
GBR16	Miniature slide switch	3	0.20	0.60	Non-specific
GBR17	Resistor 10 kOhm	3	0.08	0.24	Non-specific
GBR18/TMS03	Wire red 0.14 mm^2	0.26 m	0.01	0.26	Non-specific
GBR19/TMS04	Wire black 0.14 mm^2	0.22 m	0.01	0.22	Non-specific
GBR20/TMS05	Wire green 0.14 mm^2	0.12 m	0.01	0.12	Non-specific
GBR21/TMS07	Wire yellow 0.14 mm^2	0.12 m	0.01	0.12	Non-specific
GBR22/TMS11	Heat-shrink 2.4 mm	0.12 m	0.01	0.12	Non-specific
GBR23	Heat-shrink 6.4 mm	0.05 m	0.01	0.05	Non-specific
GBR24	M3 Nylon Hex Spacer 10 mm	1	8.99	8.99	Non-specific
GBR25	Pin header male	1	0.03	0.03	Non-specific
GBR26/TMS17	ABS filament white (*Part_8*, *Part_9*)	5.88 m	0.15	0.88	ABS
		Grand total		**72.53** €	

5.1. Tree response sensor

The description below explains the assembly of TRS step by step:

1. Print *Part_1* to *Part_6* using white ABS filament. The white color minimizes the sensor housing's unwanted heating when exposed to sunlight. Print *Part_7* using transparent ABS filament.

2. Take the pin header from the GY9250 module (*TMS02*) and break off a piece of four pins. Solder this pin header to the pins RST, A0, D0, and D5 of the D1 mini-board (*TMS01*). Shorten the four pins to the black sockets' height, then remove the four sockets.

3. Add a 2.5 cm long piece of heat-shrink (*TMS11*) to the cathode of the LED (*TMS10*) and a 1.5 cm long piece of heat-shrink to the anode of the LED. Solder the cathode of the LED to G and the anode to pin D8 on the D1 mini-board. The cables (*TMS03* to *TMS06*) are soldered to the pins (VCC, GND, SCL, SDA) of the GY9250 module. Solder the GY9250 module to the D1 mini-board (*TMS01*) (Fig. 3).

Table 5
Bill of materials required to assemble the power supply and install TreeMMoSys.

ID	Component	Quantity	Unit	Total (€)	Material type
PSI01	Junction box 100 × 100 × 40 mm	1	0.81	0.81	Non-specific
PSI02	Power distributor block	1	5.74	5.74	Non-specific
PSI03	Terminal block	1	1.12	1.12	Non-specific
PSI04	Twin-stranded wire 0.75 mm^2	1	15.30	15.30	Non-specific
PSI05	Step down module	1	3.00	3.00	Electronics
PSI06	Heat-shrink 12.8 mm	0.04 m	0.01	0.02	Non-specific
PSI07	Power supply 12 V	1	9.26	9.26	Electronics
PSI08	Twin-stranded wire 0.14 mm^2	1	16.18	16.18	Non-specific
PSI09	Ferrules 0.25 mm^2	1	0.53	0.53	Non-specific
PSI10	Heat-shrink 2.4 mm	0.03 m	0.01	0.03	Non-specific
PSI11	USB cable A to micro B	1	4.47	4.47	Non-specific
		Grand total		**56.46** €	

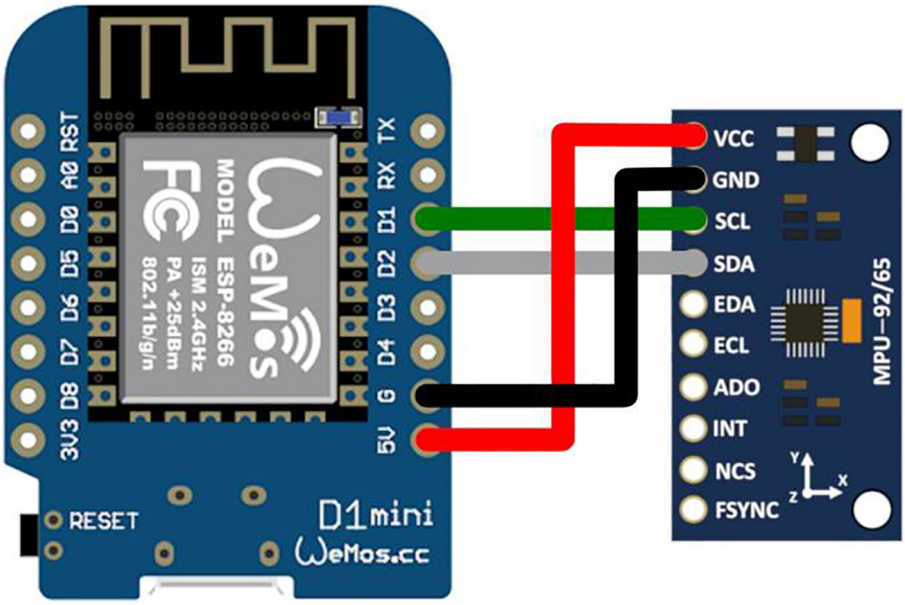

Fig. 3. Wiring diagram of MPU9250 and D1 mini-board. Figures are adopted and modified from [23,24].

4. Place the GY9250 module in the mount MPU9250 (*Part_4*) and put the mount on the D1 mini-board so that both parts on the long side opposite the USB connector are flush. Stick a piece of 1.0 cm foam (*TMS12*) on top of the GY9250 module and put the stack into sensor housing (*Part_1*). The piece of foam prevents the stack from moving within the housing due to vibrations and shocks.

5. Take the ball head (*Part_5*) and mount base (*Part_6*), and press the ball head into the base using a water pump pliers. Try to keep both parts as straight as possible in the pliers; otherwise, the ball head may break when force is applied. Stick a 2.5 cm long piece of foam onto the smooth side of the mount base (*Part_6*). This foam piece ensures a more stable seat of the sensor on the tree and avoid slipping. Set the M3 nut (*TMS16*) into one side of the mount base (*Part_6*) and screw in the M3 × 14 mm screw (*TMS14*), including one of the washers. Connect the ball head's upper end with the sensor housing using the M3 × 22 mm screw and a washer on each side.

6. Take the lid sensor housing (*Part_2*) and LED lid (*Part_7*), and glue the LED lid into the round opening of *Part_2* so that the sealed side of the LED lid is on the outer side of the lid. Any ABS-suitable glue can be used for the adhesive connection or acetone can be used to weld the two parts together.

7. Solder a 15 cm long piece of twin-stranded wire 0.14 mm^2 (*TMS08*) to the micro USB plug (*TMS09*). Positive (+) wire to pin 1 and negative (−) wire to pin 5. Set the micro USB plug into the lid of the sensor housing (*Part_2*) and slide the cable cover (*Part_3*) over the ends of the wire. Add some liquid rubber (*TMS19*) around the USB plug to seal the connection and slide the cable cover entirely over the USB plug. If necessary, also add some liquid rubber around the joint between the lid of the sensor housing and the cable cover.

8. Connect the D1 mini-board to your computer using the USB cable (*PSI11*) and load script "Calibration_Mag_MPU9250.ino" onto the board. Open the serial monitor, change the baud rate to 115,200 and follow the instructions on the screen. Note the bias and scale factors of the magnetometer for the X-, Y-, and Z-axis.

9. Download and open "TRS_MPU9250.*ino*" script provided online (https://doi.org/10.17605/OSF.IO/J63V5) and change the following values:

a. WLAN_SSID: WLAN SSID of your ground receiver
b. WLAN_PASS: WLAN password of your ground receiver
c. MQTT_SERVER: IP address of your ground receiver
d. ID: integer (sensor identification)
e. hxb: X-axis bias of magnetometer
f. hxs: X-axis scale factor of magnetometer
g. hyb: Y-axis bias of magnetometer
h. hxs: Y-axis scale factor of magnetometer
i. hzb: Z-axis bias of magnetometer
j. hxs: Y-axis scale factor of magnetometer

If multiple ground receivers are used, WLAN SSID, WLAN password, and MQTT_SERVER IP address need to be changed for each system individually. For each TRS, an individual ID has to be assigned; otherwise, no distinction can be made between different sensors' data.

10. When TRS is assembled, it can be set into the sensor housing, and the connection between the sensor lid and sensor housing can be sealed using liquid rubber. If changes have to be made to the script, carefully open the case by levering it using a screwdriver. Fig. 4 shows an assembled TRS mounted to the stem of a Scots pine tree.

5.2. Ground receiver

This part describes the assembling steps for the ground receiver. The steps are equal for V1 and V2.

1. 3D print the panel ground receiver (*Part_8*) using white ABS filament or any other filament.
2. Take the circuit board (*GBR08*) and cut a piece with 15 × 4 rows of complete soldering points out of it, and solder five JST pin headers (*GBR07)* on it. The circuit board serves as a power connector for the ground receiver. Depending on your demands, connect up to four ground receivers to the circuit board, but in this case, a large junction box is needed. Connect all left and right JST pin headers by creating separated soldering tracks. Take a 4.0 cm long slice of the single-side self-adhesive foam (*GBR09*) and stick it onto the soldering tracks to prevent short circuits.
3. Take one JST connector with a cable (*GBR07*) and solder it directly onto the test point at the backside of the power (PWR) plug of the Raspberry Pi Zero W (*GBR01)*. The correct position of these solder points (VCC and GND) is shown in the online photo series. Take a 1.0 cm long slice of the single-side self-adhesive foam (*GBR09*) and stick it onto the solder connections to prevent short circuits.
4. Cut off five pins from the pin header (*GBR25*) and solder them to the pins 1, 3, 5, 7, and 9 of the Raspberry Pi Zero W. Connect the RTC (*GBR11*) to these pins.
5. Take 6.0 cm long pieces of wire (*GBR18-GBR21*), the 10 kOhm resistor (*GBR17*), and connect them to two of the slide switches (*GBR16*) (Fig. 5). Cover soldering joints and blank wires with the heat-shrink (*GBR22*). Bundle the cables using a 1.0 cm long piece of heat-shrink (*GBR23*). Detailed pictures for the wiring are provided in the photo series online. Connect the red wire (3.3 V) to pin 17, black wire (GND) to pin 39, yellow wire to pin 37 (GPIO 26), and the green wire to pin 35 (GPIO 19) on the Raspberry Pi Zero W.

Fig. 4. Tree response sensor (TRS) mounted to the stem of a Scots pine tree.

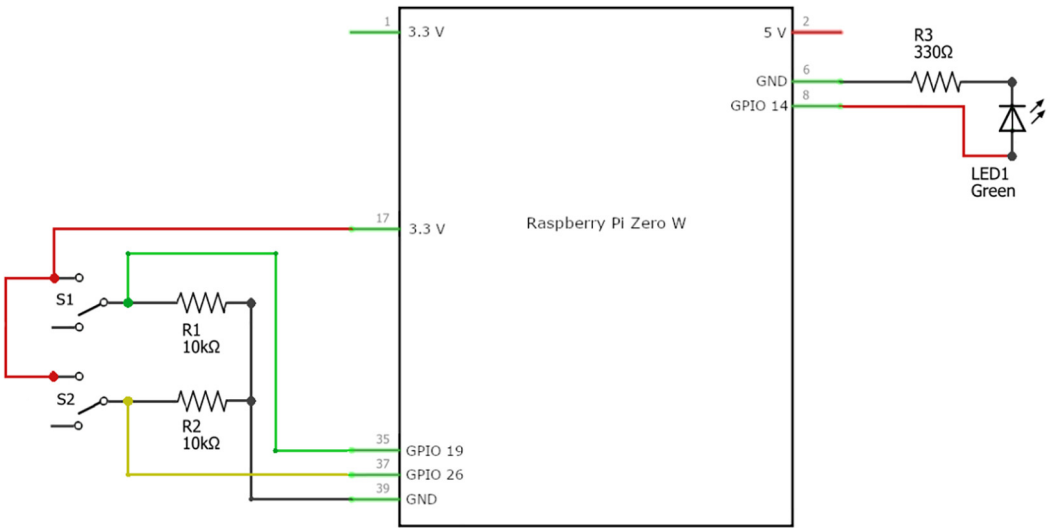

Fig. 5. Wiring diagram of the ground receiver.

6. Take the LED (*GBR14*) and solder the 330 Ohm resistor (*GBR15*) to one end of it, and solder 4.0 cm long pieces of red and black wires (*GBR18*, *GBR19*) on it. Use the 2.4 mm heat-shrink (*GBR22*) to seal the soldered joints. Connect the black wire to pin 6 (GND) and the red wire to pin 8 (GPIO 14) on the Raspberry Pi Zero W.
7. Set the switches and the LED into the panel (*Part_8*). If necessary, glue the switches and the LED to the panel with hot glue. Label the switch connected to the green cable "USB" and the switch connected to the yellow cable "Shut-down". Connect the panel to the Raspberry Pi Zero W using the 1.0 cm long nylon spacers (*GBR24*) and the USB adapter (*GBR13*) to the USB port.
8. For the power supply, take the step-down module (*GBR04*) and solder a 7.0 cm long piece of twin-stranded wire 0.75 mm^2 (*GBR06*) to the positive (+) and negative (-) input pins and connect the terminal block (*GBR10*) to the other end of the wires. Take the JST connecter with cable (GBR07) and solder the wires to the step-down module's output pins. Use a 4.0 cm long piece of 12.8 mm heat-shrink (*GBR05*) to cover the step-down module's electronic parts and avoid short circuits.
9. Connect the Raspberry Pi Zero W and step-down module to the circuit board using the JST connectors. Cut one inlet of the junction box (*GBR03*) open and place the ground receiver into it. Fig. 6 shows the assembled ground receiver.

5.3. WLAN access point

This section describes the assembly of the WLAN access point. The instructions largely correspond to the instructions for assembling the ground receiver. Therefore, only significant changes from the instructions of the ground receiver are given. For all other steps, please refer to the previous descriptions.

1. Print *Part_9* using white ABS filament or any other filament.
2. Repeat instructions 2 and 3 from the ground receiver assembling.

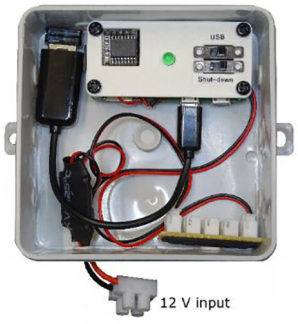

Fig. 6. Top view on the ground receiver.

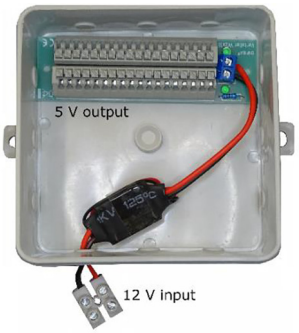

Fig. 7. Power distribution box for the tree response sensors (TRS).

3. Repeat instructions 5 to 10 from the ground receiver assembling, but use only one slide switch (*GBR16*) instead of two. Connect the green wire (*GBR20*) to pin 35 (GPIO 19) on the Raspberry Pi Zero W. At step 7, use the panel (*Part_9*) and label the switch "Shut-down".

5.4. System power supply

Connect the terminal blocks (input voltage) of the ground receiver and the WLAN access point to the 12 V DC power supply (*PSI07*). The integrated step-down modules (*GBR04*) will convert the voltage from 12 V down to 5 V. Up to 18 TRS can be connected to one power distribution box:

1. From the 0.75 mm^2 twin-stranded wire (*PSI04*), cut off two 7.0 cm long wires and solder them to the step-down module (*PSI05*) and connect the wires of the output side of the step-down module to the terminal block of the power distribution block (*PSI02*). Cover the step-down module with a 4.0 cm long piece from the 12.8 mm heat-shrink (*PSI06*).
2. Open one outlet of the junction box (*PSI01*), put all components into the junction box, lead out the power distribution box's input wires, and connect the terminal block (*PSI03*) to the wires. Fig. 7 shows the assembled power distribution box.

5.5. Software setup

Software preparation of the ground receiver and WLAN access point starts with the basic configurations of the Raspbian stretch lite image. Finish the preparation by choosing either V1 or V2. Instructions to configure the SD-card image for V1 and V2 are provided online:

1. Configuration of Raspbian image: https://doi.org/10.17605/OSF.IO/J63V5
2. Configuration of V1 ground receiver: https://doi.org/10.17605/OSF.IO/J63V5
3. Configuration of V1 WLAN access point: https://doi.org/10.17605/OSF.IO/J63V5
4. Configuration of V2 ground receiver with an integrated WLAN access point: https://doi.org/10.17605/OSF.IO/J63V5

6. Operation instructions

6.1. Tree response sensor

TRS can be mounted to the stem or branches using a cable tie. The long side (Y-axis) of the sensor head should be heading to north, and if possible, align the sensor head horizontally as precisely as possible. Fix the position of the sensor head by tightening the M3 screws. Connect TRS to a 5 V power supply using a power distribution box. Multiple power distribution boxes can be mounted to the stem at different heights on larger trees, using cable ties. TRS's external power cables can be connected to a twin-stranded wire 0.14 mm2 (*PSI08*) with the specific length to reach the power distribution box. The twin-stranded wire can be connected to TRS using ferrules 0.25 mm^2 (*PSI09*) and covered with 2.4 mm heat-shrink (*PSI10*) to avoid short circuits.

Connect the extended cable's free ends to the power distributor block (*PSI02*) within the power distribution box. Connect a 12 V power source to the power input of the distribution box. Then, TRS will connect automatically to the WLAN access point. Tree motion data will be sent via the network to the corresponding ground receiver. TRS can be disconnected and reconnected to the power supply at any time. There is no controlled shut-down necessary. As long as there is no connection to the WLAN network, the indicator LED on TRS will flash. It will turn off if the connections are established successfully.

6.2. Ground receiver

The ground receiver can be mounted to the stem at breast height (*DBH*, 1.3 m a.g.l.) using cable ties. To power the ground receiver, it needs to be connected to a 12 V power supply. For V1 systems, as soon as a connection to the WLAN access point is created, the ground receiver will automatically start to store data. The data is stored in separate files of 10-minute length within the data folder on the internal storage (SD-card) of the Raspberry Pi Zero W.

After power-up, the ground receiver of V2 will create a WLAN access point. Data will be received and stored in the internal storage as soon as TRS is connected. Display the WLAN access point in the WLAN network tab of your computer or mobile phone.

To check if data is received from TRS, establish a connection to the ground receiver by creating an SSH connection using Putty. After successfully login, enter "*sudo python test.py*", and all incoming data from TRS will be visible on the screen. After midnight (00:10), all tree response files will be copied automatically into the USB memory stick's data folder. To remove the USB memory stick from the ground receiver, use the "USB" switch to eject the connected USB device. The green indication LED will be turned on as long as you keep the switch in this position. After replacing the he USB memory stick with an empty one, turn back the "USB" switch.

There are two options to shut down the system. Firstly, by using the "Shut-down" switch on the ground receiver. Secondly, by establishing an SSH connection. If the shut-down switch is activated, the indicator LED will flash for about four seconds. Within this time, cancel the shut-down process by turning the switch back into its original position. Otherwise, the system will be turned off. To avoid damage to the SD-card image, the power supply should only be disconnected when the built-in LED on the Raspberry Pi Zero W turns off completely.

6.3. WLAN access point

For larger trees, mount the WLAN access point to the stem at a higher position. The WLAN access point needs to be connected to a 12 V power supply to power the system. The system will automatically boot and create a WLAN access point. The network should be visible in the WLAN network tab on your computer or mobile phone. All other devices, the ground receiver, and TRS will connect automatically to the WLAN network. Data will be transferred as soon as a connection is established.

To shut the WLAN access point down, there are two options. Firstly, connect and login to the WLAN access point using Putty and enter "*sudo halt*". Secondly, by shutting down the system using the "Shut-down" switch installed on the panel. The system can handle power interruptions, but in some cases, damage to the installed software images can occur, and a new installation of the image on the SD-card will be necessary. Clean system shutdowns are recommended.

7. Validation and characterization

7.1. Simulation of predefined tilt angles in the laboratory

Under laboratory conditions, TRS was mounted to a goniometer (type Winkeltronic, Nedo, Germany), tilted by predefined angles (*WRef*), and calibrated. Tilt angles (WM_d, $d = \{X,Y\}$) were measured using a digital protractor (type TLL-90S, JINGYAN Instruments & Technology, China) with an accuracy o ± 0.005°. The X- and Y-axis of the sensor were tilted in steps of 2.0° from *WRef* = 0.0° to *WRef* = 20.0° in positive and negative directions. At each step, 400 measurements were made. The zero offsets in the initial position were removed from all measured angles. Measurements below and above the 10th and 90th percentiles were omitted. 2rd polynomials were fitted to the mean tilt values of the reference and the mean measured angles to calibrate TRS. Positive and negative tilt angles were calibrated separately.

7.2. Airflow and stem tilt measurements

Airflow and stem tilt were measured between 10 April and 10 October 2020 at the forest research site Hartheim of the University Freiburg, located in the flat southern Upper Rhine Valley (47°56′04″N, 7°36′02″E). At the time of the measurements, the Scots pine forest at the research site had a mean stand density of 580 trees per hectare and a mean stand height of 18.3 m. Stem tilt was measured on three Scots pine (*Pinus sylvestris* L.) trees (T1-T3) with the height (h_i, i = 1, 2, 3) of h_1 = 17.2 m, h_2 = 17.7 m, and h_3 = 18.0 m andDBH_1 = 22.6 cm, DBH_2 = 25.8 cm, and DBH_3 = 22.8 cm. One TRS was mounted to the stems of T1-T3 at a height of 2.6 m, this corresponds roughly with the height of the first antinodal point of vibration of a clamped-free beam [29,30]. The sampling frequency of TRS was 20 Hz.

Airflow was measured close to the mean stand height using an ultrasonic anemometer (type 81000VRE, R.M. Young Company, USA) The ultrasonic anemometer was mounted on a 30.0 m high scaffold tower. The distances between T1-T3 and the tower's center were 4.4 m, 4.6 m, and 2.9 m. Airflow was measured with a sampling frequency of 10 Hz.

7.3. Data processing

The momentum flux (M) was used to capture the dynamics of the wind loads acting on T1-T3 [13,14]. Tree-specific M_i was calculated from the wind vector components measured in east–west (u), north–south (v), and vertical (w) directions as:

$$M_i = \sqrt{(u_i w_i)^2 + (v_i w_i)^2} \tag{1}$$

with u_i, v_i, and w_i being the fluctuations of the wind vector components resulting from the Reynolds decomposition.

Stem tilt data were resampled to a frequency of 10 Hz. The data of all motion axes were smoothed using a 1D Gaussian filter function from Python's SciPy package [25]. A complementary filter was applied to integrate the sensor readings of the gyroscope and accelerometer from X- and Y-axis motion data. The complementary filter is defined as [27]:

$$\theta_{Angle} = \alpha \cdot \left(\theta_{Angle} + \omega_{Gyro} \cdot dt\right) + (1 - \alpha) \cdot a_{Acc} \tag{2}$$

with θ_{Angle} being the X- and Y-axis tilt angles, ω_{Gyro} represents the angular velocity from gyroscope measurements, dt is the time difference between consecutive measurements, and α represents the filter coefficient. From laboratory tests, a value of $\alpha = 0.25$ yielded the best reproduction of the tilt angles. a_{Acc} are the angles calculated from accelerometer measurements [28] calculated here for the X- and Y-axis as

$$a_{Acc,X} = tan^{-1}\left(\frac{A_X}{\sqrt{A_Y^2 + A_Z^2}}\right)$$

$$a_{Acc,Y} = tan^{-1}\left(\frac{A_Y}{\sqrt{A_X^2 + A_Z^2}}\right) \tag{3}$$

with A_x, A_y, and A_z being the acceleration values in X-, Y-, and Z-directions.

Before calculating the tilt angles in X- (θ_X) and Y-directions (θ_Y), the 10 min means of θ_X and θ_Y were removed. The code for preprocessing the motion raw data is available online: https://doi.org/10.17605/OSF.IO/J63V5.

From θ_X and θ_Y, the tilt vector (D_i) was calculated according to earlier studies [13,14]:

$$D_i = \sqrt{\theta_{X,i}^2 + \theta_{Y,i}^2} \tag{4}$$

For detailed analyses of the wind-induced tree response, time series of D_i were segmented into intervals free of change points using the R *changepoint* package [31,32]. A minimum interval length of 4000 samples (approx. 6.67 min) was applied and change points were detected by a change of D_i in mean and variance. For each interval, the mean tilt angles $\overline{D}_{i,j}$ for T1-T3 and mean momentum flux ($\overline{M}_{i,j}$) were defined. To define the mean sample tree specific sensitivity of T1-T3 to a change in $\overline{M}_{i,j}$, 3rd polynomials were fitted to $\overline{D}_{i,j}$ and $\overline{M}_{i,j}$. The resulting functions explain the change of $\overline{D}_{i,j}$ as a function of $\overline{M}_{i,j}$. The y-axis intercept gives the sensor-specific sensitivity.

To compare the wind-induced tree response at different levels of $\overline{M}_{i,j}$, all intervals were assigned to the three tree-specific mean momentum flux classes ($MC_{i,k}$, $k = 1, 2, 3$), $MC_{i,1}$: $\overline{M}_{i,j} < 0.16$ m^2/s^2 (low wind loading), $MC_{i,2}$: 0.16 m^2/s^2 $\leq \overline{M}_{i,j} \leq$ 0.85 m^2/s^2 (medium wind loading), and $MC_{i,3}$: $\overline{M}_{i,j} > 0.85$ m^2/s^2 (strong wind loading).

For each tree, a Fourier transform was applied and power spectral densities were derived using the *signal.welch* function from Pythons SciPy signal processing toolbox [25]. To ensure that each Fourier power spectra were comparable to each other the spectra were normalized [26]. Normalized Fourier power spectra were calculated for all intervals and the mean Fourier power spectra for $MC_{i,1}$, $MC_{i,2}$, and $MC_{i,3}$ were computed.

7.4. Results

Root mean square errors (*RMSE*), mean absolute errors (*MAE*), and mean percentage errors (*MPE*) of pre-calibration tilt angles, are given in Table 6. Pre-calibration MPE ranges between −0.75%-3.20%. The 2rd polynomial equations (forced through zero) resulting from the calibration of WM_d to *WRef*, the associated coefficient of determination (R^2), *RMSE*, *MAE*, and *MPE*, are also listed in Table 6. The R^2 values of 1.000 and the values of *RMSE*, *MAE*, and *MPE* close to zero, indicate that the calibration improved the accuracy of TRS in reproducing *WRef*.

To demonstrate the performance of the TRS during long-term monitoring under field conditions, data from 184 consecutive days were used. Fig. 8 shows the averaged 10 min tilt angles of $\overline{D}_{1,j}$-$\overline{D}_{3,j}$ for a total of 26,496 intervals. Long term data showed only a low daily drift for periods of low momentum flux (T1-T3 < 0.00001°).

For more complex analyses of the wind-induced tree response, three consecutive measurement days were selected (4–6 June 2020). On these days, the mean momentum flux was 0.85 m^2/s^2 and the highest instantaneous value of the momentum

Table 6
Pre-calibration, root mean square error (RMSE), mean absolute error (MAE), and mean percentage error (MPE) calculated from the comparison of measured tilt angles D_i, and reference tilt angles (*WRef*) in *X*- and *Y*-direction. Polynomial fit equations (forced through zero), coefficient of determination (R^2), *RMSE*, *MAE*, and *MPE* calculated from the comparison of calibrated tilt angles (WM_d), and *WRef*.

Axis	Pre-calibration *RMSE*(°)	*MAE*(°)	*MPE*(%)	Post-calibration Polynomial fit	R^2	*RMSE*(°)	*MAE*(°)	*MPE*(%)
+*X*	0.281	0.281	3.204	$0.0008 \cdot D_i^2 + 0.9618 \cdot D_i$	1.000	0.006	0.017	0.191
−*X*	0.093	0.097	−0.829	$0.0006 \cdot D_i^2 + 0.9988 \cdot D_i$	1.000	0.005	0.011	−0.116
+*Y*	0.157	0.159	1.904	$0.0004 \cdot D_i^2 + 0.9789 \cdot D_i$	1.000	0.001	0.017	0.208
−*Y*	0.091	0.095	−0.749	$0.0006 \cdot D_i^2 + 0.9989 \cdot D_i$	1.000	0.006	0.011	−0.076

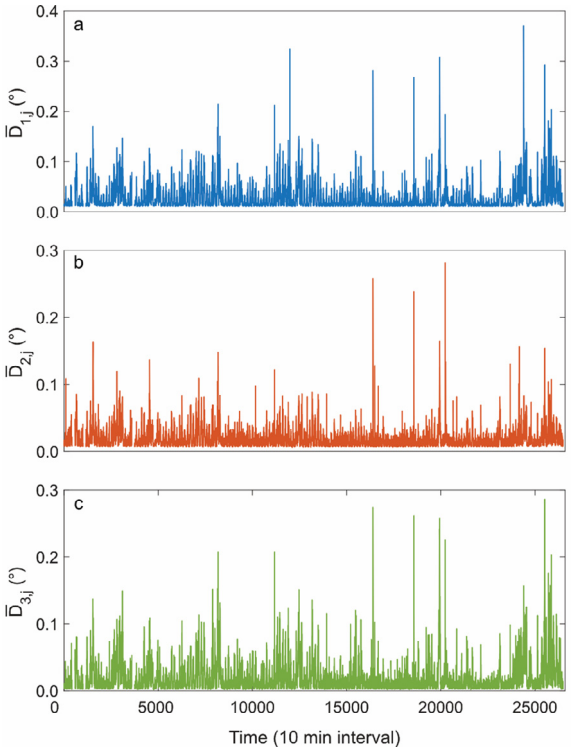

Fig. 8. Long-term time series of 26,496 intervals of averaged 10 min stem tilt ($\overline{D}_{1,j}$-$\overline{D}_{3,j}$), for the period of 10 April until 10 October 2020.

flux was 102.1 m^2/s^2. At T1-T3, TRS noise ± standard deviation in rest position was 0.02° ± 0.002° up to the 99th percentile. The mean sensitivities for T1-T3 are summarized in Table 7.

The mean tilt ± standard deviation of stems of T1-T3 in response to the wind loading were 0.05° ± 0.06°, 0.04° ± 0.04°, and 0.05° ± 0.06°. The sample tree-specific maximum 10 Hz tilt angles being 1.95°, 1.83°, and 1.52°. Fig. 9 shows the development of $\overline{D}_{1,j}$, and $\overline{M}_{1,j}$ during the period of investigation. It is obvious that $\overline{D}_{1,j}$ closely follows $\overline{M}_{1,j}$. The tilt of the stem of T1 was most pronounced in the afternoon of 5 June when wind loading was strongest. In the periods when the wind loading is very

Table 7
Polynomial fit equations calculated from the comparison of mean stem tilt ($\overline{D}_{i,j}$) as a function of mean momentum flux ($\overline{M}_{i,j}$) for T1-T3 (i = 1,2,3) in the irregular intervals (j).

Sample tree	Polynomial fit
T1	$D_{1,j} = -0.0012 \cdot \overline{M}_{1,j}^3 + 0.0096 \cdot \overline{M}_{1,j}^2 + 0.0318 \cdot \overline{M}_{1,j} + 0.0164$
T2	$D_{2,j} = -0.0004 \cdot \overline{M}_{2,j}^3 + 0.0079 \cdot \overline{M}_{2,j}^2 + 0.0083 \cdot \overline{M}_{2,j} + 0.0218$
T3	$D_{3,j} = -0.0018 \cdot \overline{M}_{3,j}^3 + 0.0124 \cdot \overline{M}_{3,j}^2 + 0.0296 \cdot \overline{M}_{3,j} + 0.0181$

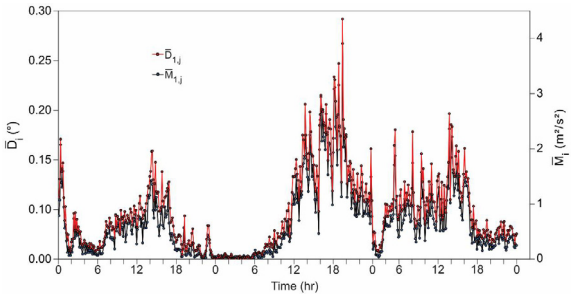

Fig. 9. Time series of mean stem tilt ($\overline{D}_{1,j}$), and mean momentum flux ($\overline{M}_{1,j}$) of sample tree T1 in 529 intervals on 4–6 June 2020.

low, stem tilt decreases to zero. Because the course of the two curves is very similar, the Pearson correlation coefficient (R) between $\overline{D}_{1,j}$ and $\overline{M}_{1,j}$ is 0.97. The same applies to T2 and T3. For these trees, R is 0.96 and 0.95.

To study the spectral response of T1-T3 to wind loading, Fourier power spectra were computed from $D_{i,j}$. The mean Fourier power spectra ($f\overline{S}_{i,k}(f)$) are presented as the product of the Fourier frequency (f) and the power spectral density ($S_{i,k}(f)$) related to $MC_{i,k}$ in Fig. 10.

In $MC_{i,1}$, where wind loading was low, $f\overline{S}_{i,1}(f)$ is similar for T1-T3. It does not show any pronounced peak that can be related to the vibration modes typically found in Fourier spectra calculated from tree motion data [33]. With increasing wind load in $MC_{i,2}$ and $MC_{i,3}$, the spectral energy is more concentrated on two narrow frequency bands. These frequency bands are associated with the first and second vibration modes of T1-T3. The dominant mean frequencies ($\overline{f}_{i,1}$) of the first vibration modes of T1-T3 are 0.273 Hz, 0.312 Hz, and 0.312 Hz. The mean frequencies dominating the second vibration mode ($\overline{f}_{i,2}$) are 0.547 Hz, 0.625 Hz, and 0.625 Hz.

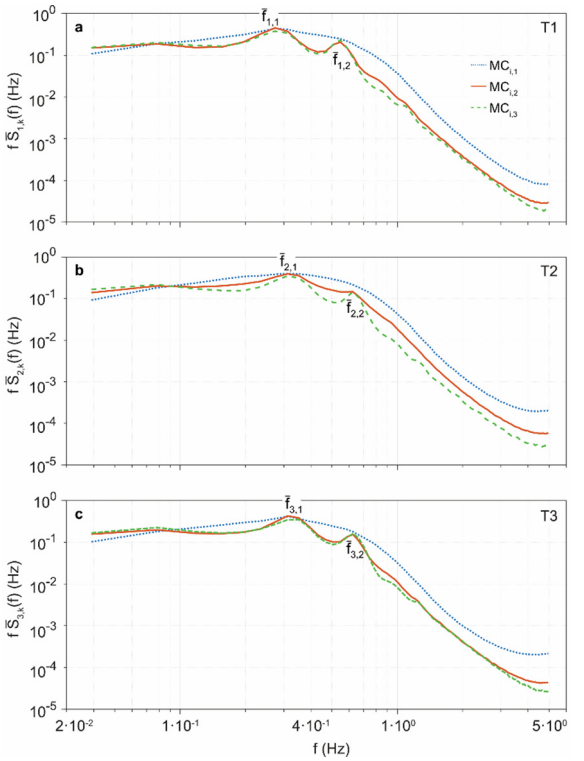

Fig. 10. Mean Fourier power spectra ($f\overline{S}_{i,k}(f)$) calculated from time series of wind-induced tilt ($D_{i,j}$) of the stem of sample trees T1-T3 for the tree-specific momentum flux classes $MC_{i,k}$. The mean frequency associated with the first and second vibration modes are highlighted by $\overline{f}_{i,1}$ and $\overline{f}_{i,2}$.

8. Conclusions

Based on the instructions summarized in this article, the tree motion monitoring system TreeMMoSys can be assembled. The weatherproof system is characterized by high portability and scalability. It enables comprehensive, long-term (tested over several months in the field) measurements of wind-induced reactions of branches and the stem. Due to its low cost and the various options for installing of tree motion sensors, it is now possible to intensively monitor the reactions of one or more full-scale trees under real wind conditions. This paper enables a widespread use of the presented system. Its use could help providing further important information necessary for a better understanding of wind-tree interaction and the formation of storm damage in forests.

Declaration of Competing Interest

The authors declare that they have no known competing financial interests or personal relationships that could have appeared to influence the work reported in this paper.

Acknowledgement

No funding was received for this study.

Appendix A. Supplementary data

Supplementary data to this article can be found online at https://doi.org/10.1016/j.ohx.2021.e00180.

References

[1] T. Wohlgemuth, M. Hanewinkel, R. Seidl, Windstörungen. In: T. Wohlgemuth, A. Jentsch, R. Seidl, (Eds.) Störungsökologie, 2019. Hauptverlag Bern, Schweiz.
[2] M.-J. Schelhaas, G.-J. Nabuurs, A. Schuck, Natural disturbances in the European forests in the 19th and 20th centuries, Glob. Change Biol. 9 (2003) 1620–1633.
[3] D. Schindler, C. Jung, A. Buchholz, Using highly resolved maximum gust speed as predictor for forest storm damage caused by the high-impact winter storm Lothar in Southwest Germany, Atmos. Sci. Let. 17 (2016) 462–469.
[4] A. Lindroth, F. Lagergren, A. Grelle, L. Klemendtsson, O. Langvall, P. Weslien, J. Tuulik, Storms can cause Europe-wide reduction in forest carbon sink, Glob. Chang. Biol. 15 (2009) 346–355.
[5] B. Gardiner, K. Byrne, S. Hale, K. Kamimura, S.J. Mitchell, H. Peltola, J.-C. Ruel, A review of mechanistic modelling of wind damage risk to forests, Forestry 81 (2008) 447–463.
[6] S.E. Hale, B.A. Gardiner, A. Wellpott, B.C. Nicoll, A. Achim, Wind loading of trees: influence of tree size and competition, Eur. J. Forest Res. 131 (2012) 203–217.
[7] B. Gardiner, B.P. Berry, P.B. Moulia, Review: Wind impacts on plant growth, mechanics and damage, Plant Sci. 245 (2016) 94–118.
[8] E. de Langre, Plant vibrations at all scales: a review, J. Exp. Bot. 70 (2019) 3521–3531.
[9] K.R. James, G.A. Dahle, J. Grabosky, B. Kane, A. Detter, Tree biomechanics literature review: dynamics, Arboricul. Urban. For. 40 (2014) 1–15.
[10] G.A. Dahle, K.R. James, B. Kane, J.C. Grabosky, A. Detter, A review of factors that affect the static load-bearing capacity of urban trees, Arboricul. Urban. For. 43 (2017) 89–106.
[11] R.B. Stull, An Introduction to Boundary Layer Meteorology (1988). Kluwer Academic Publishers.
[12] T. Foken, Micrometeorology (2017). Springer-Verlag.
[13] D. Schindler, M. Mohr, Non-oscillatory response to wind loading dominates movement of Scots pine trees, Agr. Forest Meteorol. 250 (2018) 209–216.
[14] D. Schindler, S. Kolbe, Assessment of the response of a Scots pine tree to effective wind loading, Forests 11 (2020) 145.
[15] J.R. Moore, B.A. Gardiner, G.R.A. Blackburn, A. Brickman, D.A. Maguire, An inexpensive instrument to measure the dynamic response of standing trees to wind loading, Agr. Forest Meteorol. 132 (2005) 78–83.
[16] K.R. James, B. Kane, Precision digital instruments to measure dynamic wind loads on trees during storms, Agr. Forest Meteorol. 148 (2008) 1055–1061.
[17] K.R. James, C. Hallam, C. Spencer, Measuring tilt of tree structural root zones under static and wind loading, Agr. Forest Meteorol. 168 (2013) 160–167.
[18] N. Angelou, E. Dellwik, J. Mann, Wind load estimation on an open-grown European oak tree, Forestry 92 (2019) 381–392.
[19] D. Schindler, J. Schönborn, H. Fugmann, H. Mayer, Responses of an individual deciduous broadleaved tree to wind excitation, Agr. Forest Meteorol. 177 (2013) 69–82.
[20] MPU-9250 Product Specification Revision 1.1. [Online]. Available: https://invensense.tdk.com/wp-content/uploads/2015/02/PS-MPU-9250A-01-v1.1.pdf.
[21] Rubfi, esp wifi repeater: A full functional WiFi Repeater. [Online]. Available: https://github.com/rubfi/esp_wifi_repeater/..
[22] Martin-ger, esp wifi repeater: A full functional WiFi Repeater. [Online]. Available: https://github.com/martin-ger/esp_wifi_repeater.
[23] Fritzing Part: WeMos D1 Mini. [Online]. Available: https://github.com/mcauser/Fritzing-Part-WeMos-D1-Mini.
[24] Maker Portal, Accelerometer, Gyroscope, and Magnetometer Analysis with Raspberry Pi Part I: Basic Readings. [Online]. Available: https://makersportal.com/blog/2019/11/11/raspberry-pi-python-accelerometer-gyroscope-magnetometer.
[25] P. Virtanen, R. Gommers, T.E. Oliphant, M. Haberland, T. Reddy, D. Cournapeau, et al, SciPy 1.0: fundamental algorithms for scientific computing in Python, Nat. Methods 17 (2020) 261–272.
[26] C. Torrence, G.P. Compo, A practical guide to wavelet analysis, Bull. Am. Meteorol. Soc. 79 (1) (1998) 61–78.
[27] P. Gui, L. Tang, S. Mukhopadhyay, MEMS based IMU for tilting measurement: Comparison of complementary and Kalman filter based data fusion. IEEE 10th Conference on Industrial Electronics and Applications (2015) 2004-2009.
[28] C.J. Fisher, Using an accelerometer for inclination sensing. AN-1057, Application note, Analog Devices (2010) 1-8. [Online]. Available: https://www.analog.com/media/en/technical-documentation/application-notes/AN-1057.pdf.
[29] D. Schindler, R. Vogt, H. Fugmann, M. Rodriguez, J. Schönborn, H. Mayer, Vibration behavior of plantation-grown Scots pine trees in response to wind excitation, Agr. Forest Meteorol. 150 (2010) 984–993.
[30] E. Simiu, R.H. Scanlan, Wind effects on structures: fundamentals and applications to design. John Wiley & Sons (1996), New York.

[31] R. Killick, I.A. Eckley, Changepoint: An R Package for Changepoint Analysis. J. Stat. W. 58 (2014) version 1.19. [Online]. Available: http://www.jstatsoft.org/v58/i03/.
[32] R. Killick, K. Haynes, I.A. Eckley, Changepoint: An R package for changepoint analysis. R package (2016) version 2.2.2. [Online]. Available: https://CRAN.R-project.org/package=changepoint.
[33] D. Schindler, Responses of Scots pine trees to dynamic wind loading, Agr. Forest Meteorol. 148 (2008) 1733–1742.